

Structural dependence of nonlinear-optical properties of methyl-(2,4-dinitrophenyl)-aminopropanoate crystals

J. L. Oudar and J. Zyss

Centre National d'Etudes des Telecommunications, 196 Rue de Paris, F-92220 Bagneux, France

(Received 22 March 1982)

We analyze the structural relationship between microscopic and macroscopic tensors which characterize the linear- and nonlinear-optical properties of molecular crystals exhibiting a strong donor-acceptor intramolecular interaction, with particular reference to methyl-(2,4-dinitrophenyl)-aminopropanoate (MAP). The quasiplanar structure of the active part of these molecules results in a strong and characteristic anisotropy of the optical hyperpolarizabilities, which can be traced up to the macroscopic level when taking into account the crystal symmetry as well as the orientation of the molecules in the unit cell. The experimental data on MAP are thoroughly analyzed on this basis, and it is found that a two-dimensional model of the lowest-order hyperpolarizability tensor results in a structural relation between the macroscopic tensor components, which is in agreement with experimental data. In addition, the principal dielectric axes of this monoclinic crystal are determined by the orientation of the aromatic plane in the unit cell. The overall analysis also enables the determination of four independent components of the molecular hyperpolarizability tensor from experimental data only, and the results have been compared to those of a semiempirical intermediate neglect of differential overlap calculation. The anisotropy of this tensor reveals that the intramolecular charge transfer responsible for the large optical nonlinearity is predominantly from the amino group to the nitro group in para position, rather than towards the nitro group in ortho position. Finally the overall analysis provides a basis for discussing what should be the best orientation of the molecules in the unit cell for maximizing the crystal nonlinearity. The result is that phase-matchable nonlinear coefficients up to six times larger than in MAP could be observed in compounds with similar molecular hyperpolarizabilities but an optimum crystal structure.

I. INTRODUCTION

The nonlinear optical properties of organic crystals have received a fair amount of interest in recent years, owing to their very large optical nonlinearities¹⁻¹³ and higher efficiency compared to the currently studied inorganic crystals.

A unique feature of these organic materials is their ability to form molecular crystals, where intermolecular forces are usually much weaker than intramolecular ones.^{14,15} As a consequence, it has become common practice to analyze, as a first approximation, the nonlinear optical susceptibility of organic crystals in terms of the nonlinear response of the molecules,^{12,16-18} neglecting any contribution due to their interactions, apart from the usual local-field correction factors.

Therefore, for a given compound, several approaches can be used concurrently, in order to gather as much information as possible on its nonlinear optical properties. For example, experimental data can be obtained through second-harmonic genera-

tion in powders,¹⁹ in liquids,²⁰⁻²⁴ or in single crystals. In order to relate the nonlinear susceptibility tensors of single crystals to the hyperpolarizability tensors of its constituent molecules, it is necessary to make use of crystal structure data. In addition, valuable insights into the origin of the nonlinearities at the molecular level can be obtained from several theoretical approaches, such as simplified models²⁴⁻²⁹ or more refined computer-assisted semi-empirical calculations.³⁰⁻³³ Since each of these approaches can only provide partial information, it is very fruitful to examine how all these results can be interrelated, so as to allow confrontation and cross-checking of all available data. In fact, few organic compounds have been studied by several independent methods, and it has been found worthwhile to perform a detailed analysis on an efficient material investigated in our laboratory, methyl-(2,4-dinitrophenyl)-aminopropanoate (MAP) (Ref. 1). In this material, as in other compounds recently demonstrated,⁴⁻¹⁰ the large second-order optical nonlinearity is due to a strong intramolecular

charge transfer between π -electron donors and acceptors interacting through a conjugated aromatic ring.^{24,25,29} As discussed in Sec. II of this paper, when this charge transfer occurs between *one* donor and *one* acceptor, the corresponding hyperpolarizability is basically a one-dimensional property directed along the charge transfer axis. However, when three radicals are involved in the charge transfer such as in MAP or in its parent molecule 2,4-dinitroaniline,²⁵ the hyperpolarizability is a two-dimensional property within the aromatic plane. As a result the linear and nonlinear dielectric tensors must reflect the orientation of the aromatic plane in the unit cell. This is readily shown for the linear optical properties, through the orientation of the principal dielectric axes, which are not determined by the crystal symmetry only. For the nonlinear optical properties, we derive in Sec. III, the geometrical relationships between the tensor components of macroscopic and molecular nonlinearities. We discuss how the above-mentioned two- or one-dimensional hypothesis can be checked from experimental data, and how the molecular nonlinearity components can be inferred from these data.

In Sec. IV, a quantitative analysis of experimental data is given for MAP, and the results are compared to those of a theoretical intermediate neglect of differential overlap (INDO) calculation. Finally, in Sec. V we discuss what should be the orientation of the molecules in the unit cell, for optimizing the crystal nonlinear susceptibility. This consideration has a practical interest, inasmuch as the crystal structure can be modified more or less independently of the molecular nonlinearity. This can be achieved by adding to a highly nonlinear molecule, properly chosen radicals^{1,4,6} which induce no basic change in the electronic structure of the donor-acceptor conjugated system, but modify the molecular geometry, the intramolecular forces, and hence the crystal structure.

II. ANISOTROPY OF THE ELECTRONIC POLARIZABILITIES OF MOLECULES WITH STRONG DONOR-ACCEPTOR INTERACTION

Before going into the details of the structural relations between macroscopic and microscopic polarizabilities, we briefly discuss in this section which qualitative features can be expected, concerning the anisotropy of the electronic linear and nonlinear polarizabilities of conjugated molecules with strongly interacting donor and acceptor groups.

Quite generally, these molecules contain a *planar* conjugated system (e.g., benzene ring, pyridine, styrene, stilbene) with several donor or acceptor substituent radicals, and the various nitroanilines constitute a typical family of such molecules.

The well-known expressions that can be derived from time-dependent perturbation theory for the linear and nonlinear polarizabilities^{34,35} will be used as a guideline for the discussion of the anisotropies and are recalled in Appendix A. These expressions involve a sum over the various excited states of the molecule, and each term of the sum is proportional to a *tensor product* of dipole matrix elements connecting the various molecular states. Among these excited states, the ones that produce the strong absorption band in the near uv, usually observed in the type of molecules we consider here, correspond to an electronic charge transfer³⁶⁻³⁹ from a donor to an acceptor radical, throughout the conjugated system. As was realized in recent years^{8,24,30,32} these electronic transitions provide the major contribution to the lowest-order hyperpolarizability of these molecules, and in fact also constitute a sizeable contribution to the linear polarizability as well, a contribution that has sometimes been termed "optical exaltation."⁴⁰ From the symmetry of these charge-transfer states, one can readily assess some important features of the anisotropy of the polarizability tensors of these molecules.

The simplest case to discuss occurs when only one donor and one acceptor are located at opposite ends of the conjugated system, as for instance in *p*-nitroaniline. In such a case, depicted in Fig. 1, there clearly is a well defined axis *a*, along which the charge transfer interaction takes place. If we neglect the out-of-plane protons of the amino group³¹ the molecular symmetry is *mm*2, hence the

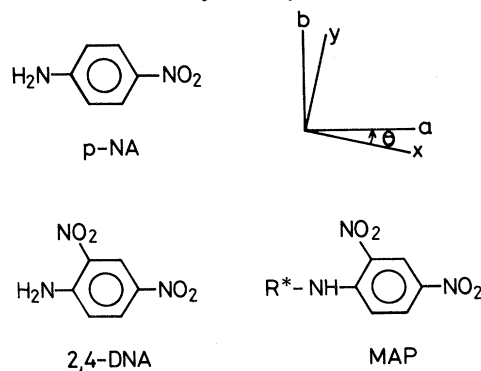


FIG. 1. Chemical formula of *p*-nitroaniline (*p*-NA), 2,4-dinitroaniline (2,4-DNA) and MAP molecules, and coordinate axes in the aromatic plane. *R** stands for (CH₃)-CH-(CO₂CH₃) chiral radical, and *x* also lies in the *XZ* plane of MAP crystal.

dipole moments, in the ground state as well as in any excited state, must be along the a axis. If we now turn to *transition* dipole moments, it can only be said from group theoretical arguments that the corresponding vectors must be either parallel to the a axis, or perpendicular to one of the mirror planes. However, for the transitions that involve an intramolecular charge transfer, the corresponding transition dipole is generally directed⁴¹ along the charge transfer axis a . These transitions involve essentially an electronic excitation from a nonbonding π -donor orbital to a π -bonding acceptor one ($n_D \rightarrow \pi_A^*$). As a result, the charge transfer contribution to the linear and nonlinear polarizabilities of this type of molecule is clearly a *one-dimensional property*, that is, the only nonzero tensor components of these polarizabilities are the ones that involve only the a subindex (α_{aa} , β_{aaa} , etc.). This feature is in fact fully confirmed by the results of detailed quantum mechanical calculations on *p*-nitroaniline.^{30,32}

We now turn to the more complex case for which a single charge transfer axis cannot so readily be defined. Representative examples of such molecules among the nitroaniline family are ortho- or meta-nitroaniline, 2,4-dinitroaniline, etc. For all these molecules, the relative positions of the substituent radicals lower the molecular symmetry, leaving only a mirror plane, parallel to the aromatic ring. The same arguments as above apply to this restricted symmetry with the result that the ground- and excited-state dipole moments are in this plane, as well as the charge transfer transition dipoles. As a consequence, charge transfer contribution to the linear and nonlinear polarizabilities of these molecules have an intrinsic *two-dimensional* character. In other words, if c is the axis perpendicular to the molecular plane, the polarizability tensor components that involve the c subindex are zero. In order to gain further insight into this problem, we have derived in Appendix A the full tensorial expression of β for a two-level system.^{8,25,42} The result involves only two vectors, the transition dipole $\bar{\mu}_{01}$ and the difference of dipole moments $\bar{\mu}_{exc} = \bar{\mu}_{11} - \bar{\mu}_{00}$ between excited and ground states. So, within this model, β is one dimensional if these two vectors are parallel to each other, and two dimensional in the other case. Quite strikingly, the limitation of the number of states involved in the nonlinear process results in a geometrical limitation on the dimensionality (in real space) of this process.

Although the preceding arguments are thought to be quite useful to predict the polarizability anisotropy, they may also be considered as an oversimplifi-

cation of the problem. So, with the aim of getting a more precise picture of these anisotropies for the MAP molecules, we have performed INDO calculations on the simpler, but closely related, 2,4-dinitroaniline molecule. These calculations are derived from a general model (LCAO-Hartree-Fock on all valence electrons) which does not require any assumption on the number of relevant eigenstates. This method can advantageously circumvent lengthy excited-state expansions of the nonlinear susceptibilities, such as classically result from a perturbational procedure. The procedure preferred here consists in a straightforward diagonalization of a semiclassical perturbed molecular Hamiltonian, including a dipolar term coupling the electrons to an external field. These calculations yield, in particular, the perturbed dipole moment of the molecule. Repetition of the same procedure at different suitable field orientations and intensities finally yields derivatives of the dipole at zero field ($d\mu'/dE$, $d^2\mu/dE^2$), corresponding to polarizability and hyperpolarizability coefficients. The INDO method⁴³ makes use of a specifically approximated LCAO-Hartree-Fock molecular Hamiltonian, including all valence electrons of the constituent atoms. It has been shown in Ref. 31 to account well for signs and relative magnitudes of lowest-order hyperpolarizabilities of aromatic substituted molecules and has also been recommended recently⁴⁴ for predicting the anisotropy of molecular polarizabilities.

As can be easily recognized from Fig. 1, the MAP and 2,4-dinitroaniline molecules are expected to possess very similar electronic properties, since they are primarily governed by the strong intramolecular charge transfer that takes place between the donor amino group (NH_2 or $\text{NH}-\text{C}_2\text{H}_4-\text{COOCH}_3$) on one hand, and the two acceptor nitro groups on the other. This similarity has been pointed out and discussed in Ref. 25 and indeed it was found that both molecules have almost identical dipole moments, near-uv absorption spectra, as well as lowest-order hyperpolarizabilities, as measured by electric field induced second-harmonic generation. This is owing to the fact that, compared to 2,4-dinitroaniline, the extra atoms which constitute the methyl-propanoate radical in MAP are quite neutral with respect to the other part of the molecule; they induce no significant perturbation into the delocalized conjugated electrons of that part and seem to bear no sizeable dipole moment by themselves.

Taking advantage of this similarity, we have performed semiempirical INDO calculations on 2,4-

dinitroaniline and calculated its dipole moment μ_i , linear polarizability α_{ij} , and lowest-order hyperpolarizability β_{ijk} using the same procedure as described in Ref. 31, namely by means of a finite-field method.

The results of this calculation can be found on Table I. The various tensor components have been expressed using the (abc) reference frame depicted on Fig. 1, with the a and b axis lying in the molecular plane, and the c axis perpendicular to it. When considering the relative values of the calculated tensor components, the most striking feature is the relative weakness of the components involving the out-of-plane c axis, especially for the hyperpolarizability tensor β_{ijk} . This fully confirms the preceding qualitative prediction that this hyperpolarizability is essentially two dimensional. This feature is not so strong for α_{ij} , which is not very surprising, since the π -electron contribution is not so prevailing for α_{ij} as it is for β_{ijk} . Inspection of the in-plane components shows that β_{aaa} is somewhat larger than the other ones, while α_{ij} is not very far from isotropic in the molecular plane.

In the next sections, the analysis of experimental data on MAP crystals will confirm these features for MAP molecules, in a completely independent way.

III. GEOMETRICAL RELATIONS BETWEEN MICROSCOPIC AND MACROSCOPIC NONLINEARITIES

In this section, we discuss the mathematical aspect of the problem with explicit reference to the monoclinic point group 2, and we point out how a lower dimensionality at the molecular level can in-

duce structural relationships between the tensor components of the crystal.

A. General expressions

As usually done, we express the lowest-order nonlinear susceptibility tensor d_{ijk} of the crystal in terms of the second-order hyperpolarizability $\beta_{ijk}^{(s)}$ of all the molecules s in a unit cell of the crystal, through the relation:

$$d_{IJK} = \frac{1}{V} f_I^{2\omega} f_J^\omega f_K^\omega \sum_s \sum_{ijk} C_{Ii}^{(s)} C_{Jj}^{(s)} C_{Kk}^{(s)} \beta_{ijk}^{(s)}, \quad (1)$$

where V is the unit cell volume, f_L^ν is a local field factor appropriate for the crystal axis L and frequency ν , and the $C_{Li}^{(s)}$ coefficients are the scalar products $\hat{L} \cdot \hat{l}(s)$ of unit vectors along crystal axis \hat{L} and molecular axis $\hat{l}(s)$.

This equation can be greatly simplified if all the molecules in a unit cell can be deduced from a particular one through the crystal symmetry operations. In that case, the molecular reference frames $l(s)_{l=1,3}$ are also deduced from a particular one through these symmetry operations. For the monoclinic point group 2, the two molecules in the unit cell are interchanged by a two-fold rotation around the Y crystal axis and Eq. (1) becomes

$$d_{IJK} = N f_I^{2\omega} f_J^\omega f_K^\omega b_{IJK}, \quad (2)$$

where

$$b_{IJK} = \frac{1}{2} \sum_{ijk} \sum_{s=1,2} C_{Ii}^{(s)} C_{Jj}^{(s)} C_{Kk}^{(s)} \beta_{ijk}. \quad (3)$$

We note that the tensor b_{IJK} , in spite of its microscopic nature, is expressed in the crystal reference frame and is submitted to the same symmetry requirements as d_{IJK} . In addition, it refers to a single average molecule, and consistently $N = 2/V$ is the number of molecules per unit volume in the crystal. Thus b_{IJK} represents the crystal nonlinear polarizability per molecule. The introduction of this tensor was found quite useful for the present purpose, and its definition can be readily generalized to all crystal point groups,⁴⁶ whatever the actual number of molecules in the unit cell. Upon the twofold rotation, the coefficients C_{Li} are multiplied by $+1$ if $L = Y$ and -1 otherwise, so that averaging over the two molecules per unit cell comes to multiply the contribution of one molecule by either 1 or 0. With the additional assumption of the Kleinman symmetry⁴⁵ the tensor d , b , and β are symmetric under any index permutation, and there remains four independent components for b , which are explicitly expressed as

TABLE I. Results of INDO calculations on 2,4-dinitroaniline (2,4-DNA).

Dipole moment	μ_a	-4.74
(in Debye units)	μ_b	-4.27
Linear polarizability	α_{aa}	23.7
(in 10^{-24} esu)	α_{ab}	0.1
	α_{bb}	19.8
	α_{cc}	4.0
Lowest-order hyperpolarizability	β_{aaa}	-6.33
(in 10^{-30} esu)	β_{baa}	0.34
	β_{abb}	2.07
	β_{bbb}	-0.43
	β_{acc}	0.08
	β_{bcc}	0.09

$$b_{YXX} = \sum_{ijk} Y_i X_j X_k \beta_{ijk} , \quad (4a)$$

$$b_{YYY} = \sum_{ijk} Y_i Y_j Y_k \beta_{ijk} , \quad (4b)$$

$$b_{YZZ} = \sum_{ijk} Y_i Z_j Z_k \beta_{ijk} , \quad (4c)$$

$$b_{YZX} = \sum_{ijk} Y_i Z_j X_k \beta_{ijk} , \quad (4d)$$

where one has chosen an arbitrary molecule in the unit cell and where, for instance, Y_i are the components in the molecular reference frame of the \hat{Y} unit vector of the crystal frame. The generalization of Eqs. (3) and (4) to other crystal point groups of interest can be found in Ref. 46.

Noting through Eq. (2) that the tensor b_{IJK} can be readily determined from the experimental data d_{IJK} measured by second-harmonic generation, we now consider under which conditions the system of Eqs. (4a) to (4d) can be solved for β_{ijk} .

In the general case of a molecule with no symmetry, the number of independent components of β_{ijk} is 10 (with Kleinman symmetry), and these individual components cannot be determined from experimental data. Strictly speaking this is the case of MAP, but as discussed in Sec. II, the active part of the molecule is a planar aromatic ring (symmetry m) with a pronounced two-dimensional character. We shall therefore consider the consequences of these properties on the structure of Eqs. (4a) to (4d). The mirror symmetry assumption restricts the number of independent components to 6, which is still too much for a complete determination of β . This number is reduced to 4 for a two-dimensional system, the components being β_{xxx} , β_{xyy} , β_{yyy} , and β_{yxx} . In the following subsection, this case is analyzed in more detail.

B. Analysis of the two-dimensional case

At first sight it may seem that the four unknown components of β can be exactly determined from the four equations (4a) to (4d). However the explicit calculation reveals that this linear system of equations is singular.

Figure 2 describes a convenient choice of coordinate systems for the crystal axes and the molecular axes. Since only the Y crystal axis is imposed by symmetry, the X axis can be arbitrarily chosen in the plane perpendicular to Y . We choose it to be also in the molecular plane, so that $X=x$ is a com-

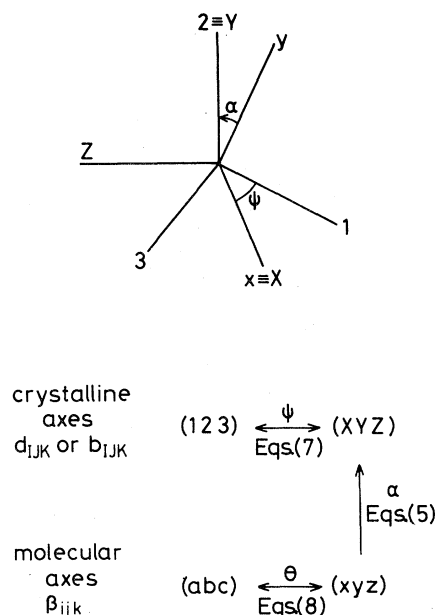


FIG. 2. Coordinate axes for the transformation between β_{ijk} and b_{IJK} (top), and summary of the geometrical transformations discussed in Sec. III B (bottom).

mon axis for macroscopic and microscopic reference frames, and call α the rotation angle around this common axis that transforms y into Y . Considering the two molecules in the unit cell, axis $X=x$ is simply the intersection of the corresponding molecular planes, and 2α is the dihedral angle between these planes. With this choice Eqs. (4a) to (4d) now take a very simple form:

$$b_{YXX} = \cos\alpha \beta_{yxx} , \quad (5a)$$

$$b_{YYY} = \cos^3\alpha \beta_{yyy} , \quad (5b)$$

$$b_{YZZ} = \cos\alpha \sin^2\alpha \beta_{yyy} , \quad (5c)$$

$$b_{XYZ} = -\sin\alpha \cos\alpha \beta_{xyy} . \quad (5d)$$

This form displays the singularity of the linear system of equations: the tensor b does not depend on β_{xxx} , which also means that this coefficient cannot be reached from second-harmonic generation data on the crystal. In addition, Eqs. (5b) and (5c) are proportional. In other words the two-dimensional assumption implies a structural relation between two components of b , namely,

$$b_{YZZ}/b_{YYY} = \tan^2\alpha . \quad (6)$$

This is a predictive relation that can readily be tested from experimental data using Eq. (2), assuming that the crystal structure is known.

Finally we note that the coordinate system sketched on Fig. 2, chosen for geometrical reasons, is not necessarily the most convenient one when discussing separately macroscopic and microscopic quantities. Conventionally, the d_{IJK} tensor is expressed in a reference frame [let us call it (123)] related to the crystallographic (or dielectric axes), and similarly a natural reference frame for discussing the hyperpolarizability tensor β_{ijk} is related to some particular atoms in the molecule, as are the a and b axes, in Fig. 1. Thus one generally needs to rotate the d_{IJK} tensor in the XZ plane and the β_{ijk} tensor

in the xy plane. These rotations are expressed as

$$d_{YXX} = \cos^2 \psi d_{211} + \sin^2 \psi d_{233} + \sin 2\psi d_{213}, \quad (7a)$$

$$d_{YYY} = d_{222}, \quad (7b)$$

$$d_{YZZ} = \sin^2 \psi d_{211} + \cos^2 \psi d_{233} - \sin 2\psi d_{213}, \quad (7c)$$

$$d_{YZZ} = \sin \psi \cos \psi (d_{233} - d_{211}) + \cos 2\psi d_{213}, \quad (7d)$$

where one goes from (XYZ) to (123) systems through a rotation of angle ψ around the $Y \equiv 2$ axis. For the two dimensional β tensor, the transformation is

$$\beta_{baa} = -\sin \theta \cos^2 \theta \beta_{xxx} + (-\sin^3 \theta + 2\cos^2 \theta \sin \theta) \beta_{xyy} + (\cos^3 \theta - 2\cos \theta \sin^2 \theta) \beta_{yxx} + \cos \theta \sin^2 \theta \beta_{yyy}, \quad (8a)$$

$$\beta_{bbb} = -\sin^3 \theta \beta_{xxx} - 3\sin \theta \cos^2 \theta \beta_{xyy} + 3\cos \theta \sin^2 \theta \beta_{yxx} + \cos^3 \theta \beta_{yyy}, \quad (8b)$$

$$\beta_{abb} = \sin^2 \theta \cos \theta \beta_{xxx} + (\cos^3 \theta - 2\sin^2 \theta \cos \theta) \beta_{xyy} + (-2\cos^2 \theta \sin \theta + \sin^3 \theta) \beta_{yxx} + \sin \theta \cos^2 \theta \beta_{yyy}, \quad (8c)$$

$$\beta_{aaa} = \cos^3 \theta \beta_{xxx} + 3\cos \theta \sin^2 \theta \beta_{xyy} + 3\cos^2 \theta \sin \theta \beta_{yxx} + \sin^3 \theta \beta_{yyy}, \quad (8d)$$

where θ is the rotation that brings the (xy) system in coincidence with any other orthogonal (ab) system, such as the one displayed on Fig. 1.

C. One-dimensional case

This case can be derived from the previous one by letting the y direction in Fig. 2 along a one-dimensional oscillator axis. Thus β_{yyy} is the only nonzero component of β , Eqs. (5b) and (5c) are unchanged; hence Eq. (6) also and Eqs. (5a) and (5d), together with Eq. (2), lead to

$$d_{YXX} = d_{YXZ} = 0. \quad (9)$$

These relations imply that if ξ is an arbitrary direction in the XZ plane, the tensor component $d_{Y\xi\xi}$, which varies sinusoidally when rotating ξ around Y , should have its maximum when ξ is along Z and a zero minimum when ξ is along X . This behavior can be tested experimentally with a fairly good accuracy, and it constitutes a characteristic signature of the one-dimensional case. Another relation, equivalent to Eq. (9), is found in terms of the (123) reference frame, using Eqs. (7a) to (7d), and reads

$$\frac{(d_{213})^2}{d_{211}d_{233}} = 1. \quad (10)$$

We note that the orientation of the one-dimensional axis need not be known for testing this relation.

D. Relations for the linear polarizabilities

Quite similarly to the previous analysis, one can relate the crystal refractive indice n_L to the linear polarizability tensor α_{ij} of the molecules, again assuming for simplicity that the intermolecular interactions have a negligible effect.

If we make use of the principal dielectric axes as a reference frame and assume a Lorentz local-field correction, one is led to the so-called Lorenz-Lorentz relation⁴⁰:

$$a_{LL} = \frac{3}{4\pi N} \frac{n_L^2 - 1}{n_L^2 + 2}, \quad (11)$$

where the diagonal tensor a_{LL} represents the average linear polarizability of the crystal per molecule, just as the b_{IJK} tensor is related to the lowest-order nonlinearity d_{IJK} . Taking now into account the crystal symmetry (monoclinic point group 2, with two molecules per unit cell), the a_{IJK} tensor is related to the molecular polarizability α_{ij} through

$$a_{IJ} = \frac{1}{2} \sum_{i,j} \sum_{s=1}^2 C_{ii}^{(s)} C_{jj}^{(s)} \alpha_{ij}, \quad (12)$$

a relation which is of course the direct analog of Eq. (3). We note that in Eq. (12) the macroscopic (I,J,K) and microscopic (i,j,k) reference frames can be chosen quite arbitrarily, which was not the case for Eq. (11). Owing to the twofold symmetry axis of the crystal, the a_{IJ} tensor has four independent components, a_{XX} , a_{YY} , a_{ZZ} , and a_{XZ} , with Y along

the twofold axis, the X direction being arbitrary in the perpendicular plane. For molecules with no symmetry at all, the α_{ij} tensor has six independent components (here we neglect the eventual contribution of optical activity, which usually is relatively small). However in many cases one of the principal axes of the α_{ij} tensor is fixed by symmetry, along a rotation axis or perpendicular to a mirror plane. This reduces the number of independent components to four. If we call z this principal axis, these components are α_{xx} , α_{xy} , α_{yy} , and α_{zz} . It turns out that the 4×4 matrix which relates the a_{IJ} components to α_{ij} components is again greatly simplified if one uses the reference frames depicted on Fig. 2, with x and X being a common axis. In that case Eq. (12) becomes

$$a_{XX} = \alpha_{xx}, \quad (13a)$$

$$a_{YY} = (\cos^2 \alpha) \alpha_{yy} + (\sin^2 \alpha) \alpha_{zz}, \quad (13b)$$

$$a_{ZZ} = (\sin^2 \alpha) \alpha_{yy} + (\cos^2 \alpha) \alpha_{zz}, \quad (13c)$$

$$a_{XZ} = -(\sin \alpha) \alpha_{xy}. \quad (13d)$$

Two comments can be made from these equations. If α_{ij} is approximately isotropic in the xy plane or if x and y are principal axes of α_{ij} , then α_{xy} is zero, and from Eq. (13d) one concludes that X and Z should be two principal dielectric axes of the crystal ($a_{XZ} = 0$). This remarkable fact is found to be verified for MAP crystals, as described in Sec. IV. The other comment is that if we make the two-dimensional assumption for α_{ij} ($\alpha_{zz} = 0$), the following relation results:

$$a_{ZZ}/a_{YY} = \tan^2 \alpha \quad (2D \text{ case}) \quad (14)$$

which, of course, can be compared to Eq. (6), and yields

$$b_{YZZ}/b_{YYY} = a_{ZZ}/a_{YY} \quad (2D \text{ case}). \quad (15)$$

In fact, none of these assumptions are necessary for inverting the system of Eqs. (13a)–(13d), and the resulting equations are

$$\alpha_{xx} = a_{XX}, \quad (16a)$$

$$\alpha_{yy} = (\cos^2 \alpha a_{YY} - \sin^2 \alpha a_{ZZ}) / \cos 2\alpha, \quad (16b)$$

$$\alpha_{zz} = (\cos^2 \alpha a_{ZZ} - \sin^2 \alpha a_{YY}) / \cos 2\alpha, \quad (16c)$$

$$\alpha_{xy} = -a_{XZ} / \sin \alpha, \quad (16d)$$

which enables us to calculate the full α_{ij} tensor from the experimental refractive indices, using Eq. (11).

IV. ANALYSIS OF EXPERIMENTAL DATA ON MAP, AND COMPARISON WITH INDO CALCULATIONS

We shall now apply the previous analysis to the second-harmonic generation (SHG) results on MAP in the crystalline state¹ as well as in solution,²⁵ making use of the crystallographic data obtained by Knossow *et al.*⁴⁷

The nonlinear coefficients of MAP crystals in Ref. 1 were expressed in a (123) direct orthogonal system with axes 1 and 2 parallel to the crystallographic axes [100] and [010], respectively. From the atom coordinates given in Ref. 47 we have calculated the angles α , θ , and ψ relating this (123) reference frame, which also appears in Fig. 2, to the (ab) axes appearing on Fig. 1, and the results are given in Table II. The molecular plane was calculated from the coordinates of the three nitrogen atoms of MAP molecules. As sketched on Fig. 1, the a axis is directed from the nitrogen atom of the amino group to the nitrogen atom of the nitro group in para position.

As already mentioned in Sec. IIID, the intersection of the XZ plane with the molecular plane is found nearly parallel to the principal dielectric axis of highest refractive index. Since this axis was named Z in Ref. 1, one has to compare ψ in this paper to $u = 37^\circ$ of Ref. 1. The agreement is within 1° , comparable to the quoted experimental uncertainty on u (0.5°). Such a coincidence can actually be inferred from Eq. (13d) and the INDO results showing near in-plane isotropy of the molecular polarizability.

To analyze the SHG results, we first expressed the d_{IJK} tensor in the XYZ axes, using Eqs. (7a)–(7d). Then we calculated the components of b_{IJK} , using Eq. (2). For simplicity we used the Lorentz local field factors

$$f_L^\nu = [(n_L^\nu)^2 + 2] / 3, \quad (17)$$

where $L = X, Y$, or Z and $\nu = \omega$ or 2ω .

In this formula, we took advantage of the near exact coincidence of the XYZ axes with the principal dielectric axes of the crystal, so that the published values of n_X , n_Y , and n_Z were directly used for the calculation of the local field factors, apart

TABLE II. Calculated values of α , θ and ψ obtained from crystal structure data (Ref. 47).

α	θ	ψ
36.89°	14.11°	36.05°

TABLE III. Components of the b tensor, derived from SHG experimental results of Ref. 1. Units are 10^{-30} esu.

b_{YXX}	b_{YYY}	b_{YZZ}	b_{YXZ}
-1.62	-3.59	-1.93	-1.12

from the above-mentioned interchange of X with Z . We use $N = 3.2 \times 10^{21}$ molecules/cm³, as calculated from the crystallographic data, and the final results for b_{IJK} are given in Table III.

Note that the overall absolute sign of the d_{IJK} tensor was not experimentally determined in Ref. 1. However, the solution measurements have shown that the scalar product $\sum_{i,j} \mu_i \beta_{ijj}$ where μ_i is the i component of the molecular dipole, is positive. From this, and from the orientation of the molecule in the crystal, we infer that the vector part of d_{IJK} should be oriented along $-Y$, in other words the sum $d_{211} + d_{222} + d_{233}$ should be negative. This condition removed the overall sign indeterminacy.

One is now in a position to test the validity of one-dimensional or two-dimensional approximations for describing the β tensor of MAP. Table IV shows the comparison between experimental and theoretical values of the quantities expressed in Eq. (6) for the two-dimensional assumption, and Eq. (10) for the one-dimensional assumption.

Obviously the one-dimensional approximation is not satisfactory, which is also indicated by the fact that the effective nonlinear coefficient displayed in Fig. 3 or Ref. 1 does not go to zero minimum when rotating the crystal around the Y axis: No X direction can be found for which Eq. (9) would be verified.

In contrast the agreement with Eq. (6) is fairly good. This result supports the two-dimensional assumption, in agreement with the theoretical findings. Therefore we shall complete the analysis of experimental data within the framework of the two-dimensional model.

The values of b_{IJK} in Table III, together with Eqs. (5a)–(5d), allow the determination of three components of β , the result of which is given in Table V. Since β_{xxx} cannot be determined by this method, one can now make use of another available

TABLE IV: Comparison between experimental and theoretical ratio of coefficients.

	Experimental	Theoretical	Hypothesis
b_{YXX}/b_{YYY}	0.54	0.56	2D
$d_{213}^2/(d_{211}d_{233})$	0.005	1	1D

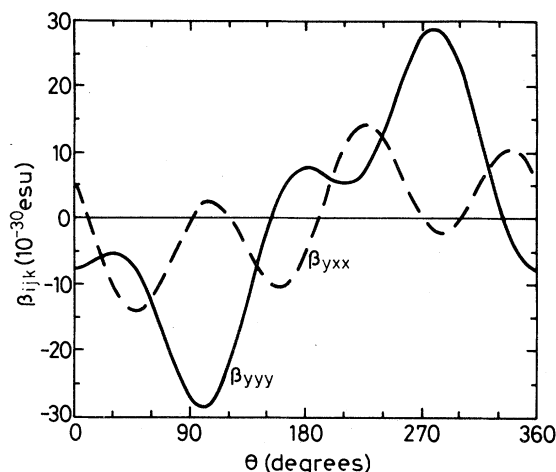


FIG. 3. Variation of the molecular β_{ijk} components upon rotation of MAP molecules in the ab plane. The numerical values are those of Table V.

experimental data, obtained on MAP in solution by electric-field-induced second-harmonic generation. This data is the projection β_μ of the vector part of β along the dipole moment direction, and its value²⁵ is $\beta_\mu = +22 \times 10^{-30}$ esu. From the results of the INDO calculations it is found that the dipole moment direction makes an angle $\eta = 222^\circ$ with the a axis. Using these results, one readily determines β_{xxx} from the relation

$$\beta_\mu = (\beta_{xxx} + \beta_{xyy}) \cos(\theta + \eta) + (\beta_{yxx} + \beta_{yyy}) \sin(\theta + \eta) \quad (18)$$

and the numerical value of this last component is also given in Table V.

One immediately notes that the largest of these components is precisely the one that does not contribute to the optical response of the crystal, which is rather unfortunate. In the next section, we shall examine in some details how much could be gained if the orientation of the molecules in the crystal were more favorable.

In order to compare these results with the INDO calculations it is necessary to express β in the (ab) reference frame, which is performed with the help of Eqs. (8a)–(8d). The results can be found on Table V. The validity of a confrontation between INDO and experimentally inferred values of β is limited by the extreme sensitivity of the tensorial coefficients, in particular the smaller ones (β_{abb} , β_{baa}), to small rotations of angle θ around c , as appears from Table V. INDO calculations have been performed on a "model molecule" of MAP, namely 2,4-dinitroaniline, with a resulting uncer-

TABLE V. Components of the two-dimensional tensor β as derived from experimental data on MAP [Eqs. (5) and (18)]. Units are 10^{-30} esu.

β_{xxx}	β_{xyy}	β_{yyy}	β_{yxx}
-28.5	+2.3	-6.8	-2.0
β_{aaa}	β_{baa}	β_{abb}	β_{bbb}
-27.1	+5.6	-0.48	-7.7

tainty on the definition of the best relative orientations of the substituent groups. This may result in a considerable discrepancy between theory and experiments on the smaller nonlinear coefficients. A common tendency showing up consistently in both calculated and experimental results is the marked anisotropy of the β tensor (i.e., β_{aaa} much larger than other coefficients) corresponding to a prevailing charge transfer in the para direction, and the negative sign of β_{aaa} (consistent with a charge transfer from the amine donor to the nitro acceptor groups). Although rather anisotropic, both experimental and theoretical β tensors exhibit a definite two-dimensional extension, as shown by the impossibility of satisfying in both cases such relations as

$$\beta_{bbb}/\beta_{aaa} = (\beta_{abb}/\beta_{baa})^3$$

demanding by a one-dimensional extension.

The refractive index data have also been analyzed along the lines of Sec. III D, taking into account the dispersion behavior, which was experimentally determined in Ref. 1, for optical wavelengths ranging from 0.509 to 1.318 μm . In order to make the best use of these data, the tensor components $a_{LL}(\lambda_p)$ were calculated using Eq. (11), at each wavelength λ_p for which the refractive indices had

TABLE VI. Linear polarizability results obtained from the refractive indices of MAP crystals. See Eqs. (11), (19), and (16). Units for $a^{(0)}$ and $a^{(1)}$ are 10^{-24} esu and for $a^{(2)}$ are 10^{-16} esu.

Sellmeier term	(0)	(1)	(2)	$\lambda_L(\mu\text{m})$
a_{XX}	32.5	5.3	0.42	0.377
a_{YY}	24.9	2.6	0.19	0.413
a_{ZZ}	22.0	1.3	0.20	0.406
a_{XZ}	$\cong 0$	$\cong 0$	$\cong 0$	
α_{xx}	32.5	5.3		
α_{xy}	$\cong 0$	$\cong 0$		
α_{yy}	28.6	4.3		
α_{zz}	18.3	-0.4		
α_{aa}	32.3	5.2		
α_{ab}	-0.9	-0.24		
α_{bb}	28.8	4.4		
α_{cc}	18.3	-0.4		

been measured. The wavelength dependence of a_{LL} has then been put in analytical form, with a least-squares fit to Sellmeier-type equations:

$$a_{LL}(\lambda) = a_{LL}^{(0)} + a_{LL}^{(1)} \frac{\lambda_L^2}{\lambda^2 - \lambda_L^2} - a_{LL}^{(2)} \lambda^2. \quad (19)$$

The result of this calculation is given in Table VI, expressed in the same reference frame as the b_{IJK} tensor in Table III. If we neglect the last term in Eq. (19), which accounts for the vibrational absorption bands in the infrared, then $a^{(0)}$ corresponds to the zero frequency limit of the *electronic* polarizability, while the $a^{(1)}$ term gives the dispersion of the first electronic absorption band in the near uv. Since this electronic transition corresponds to the intramolecular charge transfer it is instructive to test the two-dimensional hypothesis on this resonant term. Indeed, the ratio $a_{ZZ}^{(1)}/a_{YY}^{(1)}$ is not very different from the value of $\tan^2\alpha$ (0.50 compared to 0.56) as predicted by Eq. (14). This is again a confirmation of the two-dimensional nature of the charge-transfer contribution to the polarizabilities. On the contrary this relation is not verified for $a^{(0)}$ term, which is not surprising since this term contains the contributions of all the higher-lying excited states of the conjugated part of the molecule, as well as the contribution of the chiral radical, which of course is not expected to be two-dimensional. Finally, the various components have been converted back to the molecular reference frame using Eqs. (16), and the numerical results are also given in Table VI. The nonphysical negative value of $\alpha_{zz}^{(1)}$ arises from the nonexact compensation of the two terms in Eq. (16c); however this component can be considered as being essentially zero.

V. OPTIMUM MOLECULAR ORIENTATION FOR MAXIMIZING THE CRYSTAL NONLINEARITY

Since the full nonlinear tensor of MAP molecules has been determined in the preceding section, we are now in a position to calculate what is the highest crystal nonlinearity that can be expected from compounds with similar molecular hyperpolarizabilities, but an optimized crystal structure. For simplicity, we discuss this optimization within the monoclinic point group 2, but this approach can be generalized to other point groups.⁴⁶

As can be seen from Eqs. (5a)–(5d) and (8a)–(8d), an optimum value of θ and α can be found for each particular tensor component b_{IJK} under consideration. We shall therefore consider

each case individually. In addition, we note, that the optimization can be carried out independently on θ and α , which simplifies considerably the analysis.

A. Optimum value of b_{YXX}

Equation (5a) indicates that the optimum value of α is $\alpha=0$, that is, when the twofold axis lies in the molecular plane. In addition we need to rotate the β_{ijk} tensor within its plane, in order to find the maximum value of $\beta_{yxx}(\theta)$. In Fig. 3 is given the variation of this component as a function of θ , using the experimentally determined β_{ijk} tensor (Table V) and the inverse of the transformation expressed in (8a)–(8d). From this we find that

$$\begin{aligned} |b_{YXX}|_{\max} &= |\beta_{yxx}|_{\max} \\ &= 14.2 \times 10^{-30} \text{ esu} \left[\begin{array}{l} \alpha=0 \\ \theta=47.6^\circ \end{array} \right]. \end{aligned} \quad (20)$$

With this molecular orientation, and from the experimental polarizability tensor α_{ij} , we estimate $n_X^\omega \simeq 1.81$ and $n_Y^{2\omega} \simeq 1.97$ which, for the same molecular packing density as in MAP ($N=3.2 \times 10^{21}$ molecules/cm³), would give, through Eq. (2) and Lorentz local-field factors,

$$(d_{YXX})_{\max} = 2.7 \times 10^{-7} \text{ esu}. \quad (21)$$

B. Optimum value of b_{YYY}

From Eq. (5b) the optimum value of α is also $\alpha=0$, but in this case we need to find the maximum value of $\beta_{yyy}(\Theta)$. The variation of this coefficient is also given in Fig. (3), and the optimum value is

$$\begin{aligned} |b_{YYY}|_{\max} &= |\beta_{yyy}|_{\max} \\ &\simeq 28.7 \times 10^{-30} \text{ esu} \left[\begin{array}{l} \alpha=0 \\ \theta=100.6^\circ \end{array} \right]. \end{aligned} \quad (22)$$

This molecular orientation yields $n_X^\omega \simeq 1.84$ and $n_Y^{2\omega} \simeq 2.03$, which would give

$$(d_{YYY})_{\max} = 6.1 \times 10^{-7} \text{ esu}. \quad (23)$$

This value is substantially larger than the best d_{YXX} value; however it is not very useful for birefringence phase-matched nonlinear interaction. We note that the optimum orientation is such that

the principal charge-transfer axis a is nearly parallel to the Y crystal axis ($\theta-90^\circ=10.6^\circ$). This situation is very close to that of 2-methyl-4-nitroaniline (MNA),⁴ for which the second-harmonic coefficient d_{XXX} has been measured to be $d_{XXX}(\text{MNA}) = 500d_{11}(\text{SiO}_2) \simeq 6 \times 10^{-7}$ esu. For the comparison, one also has to note the difference in molecular packing density [$N=5.5 \times 10^{21}$ molecules/cm³ in MNA (Ref. 5)]. The simpler structure of MNA accounts for the more favorable value of N .

C. Optimum value of b_{YZZ}

From Eq. (5c) we see that the optimum value of α is obtained for $3\cos^2\alpha-1=0$, i.e., $\alpha \simeq 54.74^\circ$, and that the best value for θ is the one that maximizes β_{yyy} . Therefore the result is

$$\begin{aligned} |b_{YZZ}|_{\max} &= \frac{2}{3\sqrt{3}} |\beta_{yyy}|_{\max} \\ &\simeq 11 \times 10^{-30} \text{ esu} \left[\begin{array}{l} \alpha=54.74^\circ \\ \theta=100.6^\circ \end{array} \right], \end{aligned} \quad (24)$$

which, together with the estimated refractive indices $n_Z^\omega \simeq 1.68$ and $n_Y^{2\omega} \simeq 1.56$ for this orientation would lead to

$$(d_{YZZ})_{\max} = 1.3 \times 10^{-7} \text{ esu}.$$

We note that the optimum values of b_{YXX} and b_{YZZ} are not very different in magnitude. This is because in the two-dimensional tensor β_{ijk} , one component is much larger than the other ones. Actually, if β_{ijk} were strictly one-dimensional ($\beta_{ijk}=0$ except for β_{aaa}), one would have

$$\begin{aligned} (b_{YXX})_{\max} &= \frac{2}{3\sqrt{3}} \beta_{aaa} \left[\begin{array}{l} \alpha=54.74^\circ \\ \theta=35.26^\circ \end{array} \right], \\ (b_{YYY})_{\max} &= \beta_{aaa} \left[\begin{array}{l} \alpha=0 \\ \theta=0 \end{array} \right] \quad (\text{1D case}), \\ (b_{YZZ})_{\max} &= \frac{2}{3\sqrt{3}} \beta_{aaa} \left[\begin{array}{l} \alpha=54.74^\circ \\ \theta=90^\circ \end{array} \right], \end{aligned}$$

and consequently the optimum values of b_{YXX} and b_{YZZ} would be equal. In fact, in the one-dimensional case there is no need to consider the molecular plane any longer, but only the angle ξ between the a and Y axes, and in either cases ($\alpha=0, \theta=35.26^\circ$, and $\alpha=54.74^\circ, \theta=90^\circ$) this angle is $\xi=54.74^\circ$, which maximizes the product

$\sin^2\xi \cos\xi$.

Finally, we note that the optimum value for d_{YXX} is 6.7 times larger than the phase-matchable coefficient d_{21} in actual MAP crystals, which shows that a significant improvement can be expected from an optimized crystal structure. As far as the d_{YYY} coefficient is concerned, the potential gain is still larger (roughly 14 times larger than the d_{22} of MAP), and in fact the actual crystal structure of MNA (Ref. 4) approaches this optimum orientation very closely, which is very useful for electro-optic applications.⁵

VI. CONCLUSION

This detailed analysis of structural relationships between microscopic and macroscopic tensors of MAP has provided new interesting information on the individual polarizability and hyperpolarizability tensor components of MAP molecule, and it has confirmed that a two-dimensional model is adequate for describing its lowest-order hyperpolarizability tensor with a fair degree of accuracy. Inspection of the in-plane anisotropy of this tensor reveals that the intramolecular charge transfer responsible for the large optical nonlinearity is predominantly directed towards the *p*-nitro group rather than towards the *o*-nitro group in this 2,4-dinitroaniline derivative. However a strict one-dimensional model does not lead to a correct prediction of the crystal-line nonlinear coefficients, because in the crystal structure of MAP the predominant charge-transfer axis *a* is nearly perpendicular ($\sim 79^\circ$) to the twofold symmetry axis. Naturally, this considerably lowers the contribution of the β_{aaa} component and enhances the relative weight of the other in-plane components. From a practical point of view, one

can conclude that the molecular orientation in MAP crystals is not particularly favorable, and phase-matchable nonlinear coefficients up to six times larger could be obtained with an optimum crystal structure. This point stresses the central importance of molecule orientation in the search of efficient nonlinear materials and should stimulate further studies in this direction.

Finally, we note that this analysis can be easily applied to any molecular crystal with point group 2 symmetry and could be used to further check the degree of generality of the two-dimensional assumption for the lowest-order hyperpolarizability of intramolecular charge-transfer molecules. Extension of this analysis to the other noncentrosymmetric point groups⁴⁶ allows us to perform similar studies on a larger variety of molecular crystals.

APPENDIX A: LOWEST-ORDER HYPERPOLARIZABILITY TENSOR IN THE TWO-LEVEL APPROXIMATION

Time-dependent quantum-mechanical perturbation theory allows us to express the nonlinear polarizability tensors^{34,35} in terms of the energies $\hbar\omega_p = E_p - E_0$ of excited states and of matrix elements $\mu_{pq}^i = \langle p | \mu_i | q \rangle$ of the dipole operator between states *p* and *q*. The hyperpolarizability tensor $\beta_{ijk}^{2\omega}$ for second-harmonic generation relates the peak amplitude $p_i^{2\omega}$ of the second-harmonic dipole to the peak amplitude E_j^ω of the fundamental electric field through the relation

$$p_i^{2\omega} = \beta_{ijk}^{2\omega} E_j^\omega E_k^\omega, \quad (\text{A1})$$

where $\beta_{ijk}^{2\omega}$ is expressed^{34,26} by

$$\beta_{ijk}^{2\omega} = \frac{1}{2\hbar^2} \sum_{p,q} \left[\mu_{op}^i (\mu_{pq}^j \mu_{qo}^k + \mu_{pq}^k \mu_{qo}^j) \frac{\omega_p \omega_q + 2\omega^2}{(\omega_p^2 - 4\omega^2)(\omega_q^2 - \omega^2)} + \mu_{op}^k \mu_{pq}^i \mu_{qo}^j \frac{\omega_p \omega_q - \omega^2}{(\omega_p^2 - \omega^2)(\omega_q^2 - \omega^2)} \right], \quad (\text{A2})$$

where the sum runs over all energy states of the system.

If we restrict this sum to only two levels, the ground state $|0\rangle$ and the excited state $|1\rangle$, there remains only four terms in this sum ($p, q = 0, 1$). It can be readily seen that the term $p = 0, q = 0$ is identically zero. In addition, each product in the term $p = 1, q = 1$ can be associated with a corresponding product of the terms $p = 1, q = 0$ or $p = 0, q = 1$, and the final result depends only on the difference $\delta_l = \mu_{11}^l - \mu_{00}^l$ between excited- and ground-state dipole moments. With this notation, and $m_l = \mu_{01}^l$ for the transition dipole moment, we get

$$\beta_{ijk}^{2\omega}(\text{2 levels}) = \frac{1}{2\hbar^2} \frac{\delta_i m_j m_k}{\omega_1^2 - \omega^2} + m_i (m_j \delta_k + \delta_j m_k) \frac{\omega_1^2 + 2\omega^2}{(\omega_1^2 - 4\omega^2)(\omega_1^2 - \omega^2)}. \quad (\text{A3})$$

From this expression, we note that the nonlinearity of a two-level system is a two-dimensional tensor,

since it involves only tensor products of the two vectors $\vec{\delta}$ and \vec{m} [any component involving the *z*

axis perpendicular to the $(\bar{\delta}, \bar{m})$ plane is zero]. Furthermore, if $\bar{\delta}$ and \bar{m} are parallel, then β is one-dimensional. Because of the two different frequency-dependent factors in (A3) the Kleinman symmetry relation is only valid in the limit of zero frequency, which reads

$$(\beta_{ijk}^{2\omega})_{\omega=0} = \frac{1}{2\hbar^2 \omega_1^2} (\delta_i m_j m_k + m_i \delta_j m_k + m_i m_j \delta_k) \quad (\text{A4})$$

and is proportional to the symmetrized tensor products $S(\bar{\delta} \times \bar{m} \times \bar{m})$. Finally, we note that Eq. (A3) exhibits a simple dispersion behavior for $i=j=k$, leading to

$$\beta_{xxx}^{2\omega} = \frac{3\delta_x m_x^2}{2\hbar^2} \frac{\omega_1^2}{(\omega_1^2 - 4\omega^2)(\omega_1^2 - \omega^2)} \quad (\text{A5})$$

- ¹J. L. Oudar and R. Hierle, *J. Appl. Phys.* **48**, 2699 (1977).
- ²A. Carenco, J. Jerphagnon, and A. Périgaud, *J. Chem. Phys.* **66**, 3806 (1977).
- ³J. M. Halbout, S. Blit, W. Donaldson, and C. L. Tang, *IEEE J. Quantum Electron.* **15**, 1176 (1979).
- ⁴B. F. Levine, C. G. Bethea, C. D. Thurmond, R. T. Lynch, and J. L. Bernstein, *J. Appl. Phys.* **50**, 2523 (1979).
- ⁵G. F. Lipscomb, A. F. Garito, and R. S. Narang, *J. Chem. Phys.* **75**, 1509 (1981).
- ⁶J. Zyss, D. S. Chemla, and J. F. Nicoud, *J. Chem. Phys.* **74**, 4800 (1981).
- ⁷M. Sigelle and R. Hierle, *J. Appl. Phys.* **52**, 4199 (1981).
- ⁸B. L. Davydov, L. D. Derkacheva, V. V. Dunina, M. E. Zhabotinskii, V. F. Zolin, L. G. Koreneva, and M. A. Samokhina, *Zh. Eksp. Teor. Fiz. Pis'ma Red.* **12**, 24 (1970) [*JETP Lett.* **12**, 16 (1970)]; *Opt. Spektrosk.* **30**, 503 (1971) [*Opt. Spectrosc. (USSR)* **30**, 274 (1971)].
- ⁹P. D. Southgate and D. S. Hall, *J. Appl. Phys.* **43**, 2765 (1972).
- ¹⁰J. G. Bergman, G. R. Crane, B. F. Levine, and C. G. Bethea, *Appl. Phys. Lett.* **20**, 21 (1972).
- ¹¹J. Jerphagnon, *IEEE J. Quantum Electron.* **7**, 42 (1971).
- ¹²V. D. Shigorin, *USSR Natl. Acad. Sci.* **98**, (1977).
- ¹³L. G. Koreneva, V. E. Zolin, and B. L. Davydov, in *Molecular Crystals in Nonlinear Optics* (Nauka, Moscow, 1975).
- ¹⁴A. I. Kitaigorodskii, *Organic Chemical Crystallography* (Consultant Bureau, New York, 1961).
- ¹⁵J. N. Murrell, in *Orbital Theories of Molecules and Solids*, edited by N. H. March (Clarendon, Oxford, 1974).
- ¹⁶D. S. Chemla, J. L. Oudar, and J. Jerphagnon, *Phys. Rev. B* **12**, 4534 (1975).
- ¹⁷N. Bloembergen, *Nonlinear Optics* (Benjamin, New York, 1965).
- ¹⁸J. A. Morrell, C. A. Albrecht, K. H. Levin, and C. L. Tang, *J. Chem. Phys.* **71**, 5063 (1979).
- ¹⁹S. K. Kurtz and T. T. Perry, *J. Appl. Phys.* **39**, 3798 (1968).
- ²⁰B. F. Levine and C. G. Bethea, *Appl. Phys. Lett.* **24**, 445 (1974).
- ²¹J. L. Oudar and H. Le Person, *Opt. Commun.* **15**, 258 (1975); **18**, 410 (1976).
- ²²B. F. Levine and C. G. Bethea, *J. Chem. Phys.* **63**, 2666 (1975).
- ²³K. D. Singer and A. F. Garito, *J. Chem. Phys.* **75**, 3572 (1981).
- ²⁴J. L. Oudar, *J. Chem. Phys.* **67**, 446 (1977).
- ²⁵J. L. Oudar and D. S. Chemla, *J. Chem. Phys.* **66**, 2664 (1976).
- ²⁶F. N. H. Robinson, *Bell. Syst. Tech. J.* **46**, 913 (1967).
- ²⁷J. L. Oudar and D. S. Chemla, *Opt. Commun.* **13**, 164 (1975).
- ²⁸B. F. Levine, *J. Chem. Phys.* **63**, 115 (1975).
- ²⁹B. F. Levine and C. G. Bethea, *J. Chem. Phys.* **37**, 516 (1976).
- ³⁰S. J. Lalama and A. F. Garito, *Phys. Rev. A* **20**, 1179 (1979).
- ³¹J. Zyss, *J. Chem. Phys.* **70**, 3333 (1979); **70**, 3341 (1979); **71**, 909 (1979).
- ³²J. A. Morrell and A. C. Albrecht, *Chem. Phys. Lett.* **64**, 46 (1979).
- ³³A. Schweig, *Chem. Phys. Lett.* **1**, 163 (1967); **1**, 195 (1967).
- ³⁴J. A. Armstrong, N. Bloembergen, J. Ducuing, and P. Pershan, *Phys. Rev.* **127**, 1918 (1962).
- ³⁵P. N. Butcher, *Nonlinear Optical Phenomena* (Ohio State University, Columbus, Ohio, 1965).
- ³⁶J. N. Murrell, *The Theory of the Electronic Spectra of Organic Molecules* (Wiley, New York, 1963).
- ³⁷V. N. Danilova and Y. P. Morozovan, *Opt. Spektrosk.* **12**, 5 (1962) [*Opt. Spectrosc. (USSR)* **12**, 12 (1962)].
- ³⁸I. Corbett, *Spectrochim. Acta A* **23**, 2315 (1967).
- ³⁹A. E. Lutskii and N. I. Gorokhova, *Opt. Spektrosk.* **27**, 917 (1967) [*Opt. Spectrosc. (USSR)* **27**, 499 (1967)].
- ⁴⁰R. J. W. Lefevre, in *Advances in Physical Organic Chemistry* (Academic, London, 1965), Vol. 3, p. 1. See also C. J. F. Böttcher and P. Bordwijk, *Theory of Electric Polarization* (Elsevier, Amsterdam, 1978).
- ⁴¹W. Liptay in *Excited States*, edited by E. C. Lim (Academic, New York 1974), Vol. 1, p. 129.
- ⁴²B. F. Levine and C. G. Bethea, *J. Chem. Phys.* **66**, 1070 (1977).
- ⁴³J. A. Pople and D. L. Beveridge, *Approximate Molecular Orbital Theory* (McGraw-Hill, New York 1970).
- ⁴⁴P. J. Bounds, *Chem. Phys. Lett.* **70**, 143 (1980).
- ⁴⁵D. A. Kleiman, *Phys. Rev.* **126**, 1977 (1962).
- ⁴⁶J. Zyss and J. L. Oudar, *Phys. Rev. A* **26**, 2028 (1982).
- ⁴⁷M. Knossow, Y. Mauguen, and C. de Rango, *Cryst. Struct. Commun.* **5**, 723 (1976).